Research Square

Preprints are preliminary reports that have not undergone peer review.
They should not be considered conclusive, used to inform clinical practice,
or referenced by the media as validated information.

# Tipping points in gut ecology: a hidden resilience deficit in industrialised microbiomes

**Ogochukwu Ofordile**

ogo@stercora.bio

MRC Unit at the London School of Hygiene & Tropical Medicine

**Article**

**Keywords:**

**Posted Date:** July 1st, 2026

**DOI:** https://doi.org/10.21203/rs.3.rs-9981104/v1

**License:** This work is licensed under a Creative Commons Attribution 4.0 International License.
Read Full License

**Additional Declarations:** Competing interest reported. O.O. is Founder and CEO of Stercora Biosciences Inc., a company developing Prevotella stercorea as a therapeutic, postbiotic, and diagnostic platform. The IHAT-GUT data and all analyses reported in this manuscript were completed independently of Stercora Biosciences. No funding from Stercora Biosciences supported this work.

# Abstract

The Western gut microbiome is widely considered healthy, yet its defining feature relative to non-industrialised populations is not a fundamentally different composition but a contracted one: lower genus-level richness, reduced functional redundancy, and increased reliance on a narrow set of keystone taxa. Ecological theory predicts that such systems operate closer to critical tipping points, where modest perturbations can trigger abrupt and difficult-to-reverse transitions. We argue that the Western microbiome exemplifies this configuration. Long-term reduction in infection pressure has favoured metabolic efficiency at the cost of distributed ecological buffering. Two independent datasets support this view. In 633 Gambian children, protection from infection is associated with higher genus-level richness (103.1 ± 25.3 vs 93.9 ± 25.5 genera, p = 0.0005, Cohen's d = 0.36), while Shannon diversity is non-significant and directionally reversed (2.272 vs 2.251, p = 0.649). At species level, *Prevotella stercorea* independently predicts reduced infection risk (incidence rate ratio 0.951, 95% CI 0.916–0.987, p = 0.008), with effects largely independent of richness. In parallel, longitudinal profiling of astronauts during spaceflight shows convergence in alpha diversity across individuals rather than a system-wide increase, occurring alongside depletion of immunologically important taxa and rising inflammatory markers. Across both settings, diversity metrics dissociate from functional protection for the same underlying reason: they capture distribution, not redundancy. Apparent gains in diversity can reflect ecological homogenisation rather than restoration of functional capacity. We propose that Western microbiomes represent a structurally fragile ecological state and outline testable predictions for microbiome-targeted interventions and disease risk interpretation.


## Resilience and redundancy in the gut microbiome

Ecological resilience - the capacity of a system to absorb disturbance while maintaining structure and function-depends on functional redundancy. Systems in which multiple taxa perform overlapping roles can tolerate species loss; those with limited redundancy are inherently closer to tipping points, where relatively small perturbations can drive transitions into alternative stable states that are self-reinforcing and slow to reverse.[1,2]

The gut microbiome exhibits these properties. Human populations cluster into relatively stable configurations dominated by *Bacteroides* or *Prevotella*, shaped by diet and environment.[3,4,5] From a resilience perspective, the relevant question is how close a configuration lies to a tipping point and how readily it recovers from perturbation - not whether it is healthy.

Industrialised microbiomes, we argue, occupy a shallower stability basin than their non-industrialised counterparts.

## A contracted ecological state

Industrialised environments have progressively reduced microbial exposure through sanitation, antibiotic use, and limited environmental contact. The resulting microbiome is characterised by lower genus-level richness (typically 70–90 genera) compared with non-industrialised populations (100–120 genera),[3,5] alongside a shift toward *Bacteroides*-dominant communities.[4]

This contraction produces two structural consequences. First, ecological function becomes concentrated in a small number of taxa, most notably *Faecalibacterium prausnitzii*, which acts as a dominant anti-inflammatory keystone. In high-richness systems, its loss can be buffered by a distributed network; in Western microbiomes, it often represents a terminal layer of defence with limited redundancy.

Second, reduced environmental microbial influx results in intermittent rather than tonic immune engagement. This produces a mucosal immune system that is well adapted to stable, hygienic conditions but less conditioned for sustained perturbation.

Together, these features define a "peacetime" ecological configuration: efficient and stable under the conditions that shaped it, but structurally fragile when those conditions change.

Table 1

**Structural features of Western and non-Western microbiomes**[3,4,5]

| Property | Western (Bacteroides-dominant) | Non-Western (Prevotella-dominant) |
|---|---|---|
| Genus-level richness | 70–90 genera | 100–120 genera |
| Keystone structure | Single dominant (*F. prausnitzii*) | Distributed network (*P. stercorea* + others) |
| Functional redundancy | Reduced | High |
| Immune engagement mode | Intermittent | Tonic |
| Response to perturbation | Keystone-dependent; loss of anchor = collapse | Network-buffered; individual losses compensated |

## Evidence from a high-pathogen environment

The IHAT-GUT cohort provides a direct test of which ecological features predict host protection. Among 633 Gambian children followed longitudinally, Day 85 microbiome composition best captured established ecological states across illness groups.[6]

Children who remained infection-free exhibited higher genus-level richness than those who developed illness (103.1 ± 25.3 vs 93.9 ± 25.5 genera; $p = 0.0005$, Cohen's $d = 0.36$), whereas Shannon diversity showed no association and a directionally reversed trend (2.251 ± 0.439 vs 2.272 ± 0.452; $p = 0.649$) (Fig. 1a,b). Predictive performance mirrored this dissociation: richness modestly discriminated illness

risk (AUC 0.605, 95% CI 0.548–0.662), whereas Shannon diversity performed near chance (AUC 0.521, 95% CI 0.463–0.578) (Fig. 1d).

This divergence is structural rather than statistical. Evenness can remain stable, or increase, in systems that have lost functional capacity, whereas genus-level richness more directly reflects the breadth of ecological roles available to the community.

At species level, *Prevotella stercorea* anchored this signal. Its abundance independently predicted reduced acute respiratory infection risk (IRR 0.951, 95% CI 0.916–0.987; $p = 0.008$ in joint models with *P. copri*), with effects that were species-specific, temporally antecedent to illness onset, and largely independent of richness (< 1% mediated) (Fig. 2a,b; Supplementary Tables 3–5).[6,7]

Importantly, these associations were context-dependent rather than uniformly anti-inflammatory. In low-WAZ children, *P. stercorea* associated with reduced CRP, whereas in higher-WAZ children it associated with elevated AGP and baseline inflammatory tone, supported by significant WAZ × P. stercorea interaction terms (BH-corrected, Family 2: four interaction tests) and reverse temporal analyses (Supplementary Tables 6 and 7). Together, these findings are more consistent with host immune-metabolic reserve-dependent immune conditioning than with simple suppression of inflammation.

Within a resilience framework, *P. stercorea* is therefore best interpreted not as an isolated protective species, but as a marker of a broader high-redundancy trophic network whose absence reflects structural loss of ecological buffering.

Within a resilience framework, *P. stercorea* is best understood not as an isolated beneficial species but as a marker of a broader high-redundancy trophic network[5] whose absence reflects a structural loss of ecological buffering (Fig. 2b; Supplementary Table 5).

## Spaceflight as a perturbation experiment

Spaceflight provides an extreme perturbation combining radiation exposure, circadian disruption, and near-complete cessation of environmental microbial input within a closed habitat.[8]

Alpha diversity (Shannon index and richness) increased during spaceflight in 4/5 astronauts (Shannon $p = 0.011$; richness $p = 0.05$), but these increases were relative to individual baselines and occurred primarily in those with lower pre-flight diversity (Fig. 3a). The astronaut with the highest baseline diversity showed no significant change across the mission.[8]

Rather than a system-wide increase, these dynamics are more consistent with convergence toward a shared in-flight ecological state (Fig. 3c). Diversity in lower-baseline individuals rose toward that of the highest-diversity individual early in flight, followed by partial decline later in the mission, suggesting transient homogenisation within a constrained environment. This pattern is plausibly driven by a

combination of dietary standardisation and microbial exchange within the closed ISS habitat, although direct transmission cannot be established from these data.

Importantly, this apparent convergence in diversity metrics occurs alongside depletion of immunologically important taxa, including *Akkermansia* and *Ruminococcus* (> 5-fold) and *Pseudobutyrivibrio* and *Fusicatenibacter* (~ 3-fold). Decline in *Fusicatenibacter* correlates strongly with increases in pro-inflammatory cytokines (Somers' D = − 0.58 to − 0.62, all $p < 0.0001$) (Fig. 3d), and viral reactivation is detected in 44% of astronauts (Fig. 3b).[8,9,10]

Thus, diversity metrics partially normalise across individuals while functional capacity deteriorates (Fig. 3a,c). The individual with the highest pre-flight diversity remains stable, consistent with greater resilience (Fig. 4c,d), whereas convergence in the remaining crew reflects constraint rather than recovery.[8]

# A hidden vulnerability

The IHAT-GUT and spaceflight findings converge on a common structural point: Western microbiomes likely operate below a richness threshold associated with ecological resilience in high-pathogen environments.[11]

The 9.2-genus difference separating protected and ill children occurs around a baseline of ~ 100 genera (Fig. 4b; Table 1). The typical Western range (70–90 genera) lies below this distribution, indicating not a marginal difference but a shift into a lower-redundancy regime.

The role of *Faecalibacterium prausnitzii* illustrates this constraint. High abundance signals that the system has not yet collapsed, not that it is deeply resilient. Standard clinical metrics assess current state rather than resilience, allowing systems to appear normal while remaining close to tipping points (Fig. 4a).

Spaceflight makes this vulnerability explicit. Convergence in diversity occurs under constraint, yet compositional degradation and immune dysregulation proceed. Recovery of diversity post-flight does not prevent transient immune consequences, indicating a shallow recovery basin.

**Testable predictions**

**1. Baseline richness predicts resilience**

Pre-perturbation genus-level richness will predict microbiome stability under extreme conditions better than Shannon diversity or single-taxon abundance.

**2. Ecological augmentation improves resilience**

Pre-conditioning with *P. stercorea* and substrates that support Prevotella-based networks will reduce functional taxon loss under perturbation, even without full restoration of non-industrialised richness levels.[5,8] Notably, colonisation capacity and immune effect are separable outcomes; the species-specific infection protection signal observed in IHAT-GUT is largely richness-independent and may reflect immune conditioning mechanisms that operate downstream of, and independently from, colonisation efficiency.

**3. Disease associations reflect redundancy**

Across populations, microbiome-associated disease risk will align more closely with genus-level richness and functional redundancy than with individual taxa, with species-level resolution revealing *P. stercorea*-specific effects underlying broader genus-level associations.[6,7,12,13,14]

## Conclusion

The Western gut microbiome is not pathological in the conventional sense. It is fragile in the ecological sense and the distinction is consequential.

Clinical metrics measure distance from disease states; ecological metrics measure distance from tipping points. A system can be clinically normal yet structurally vulnerable, and accumulating evidence suggests this is the case for industrialised microbiomes.

The genus-level richness and distributed immune-activating architecture characteristic of non-industrialised microbiomes are not incidental features. They are structural components of resilience that industrialisation has progressively reduced.[3,4] Their absence becomes visible only under perturbation, but when revealed its consequences are measurable.[15]

The priority is therefore not only to describe microbiome composition, but to quantify resilience and restore it where possible. Genus-level richness and functional redundancy are measurable, actionable, and when lost consequential.

Among candidate interventions, *Prevotella stercorea* is particularly well-positioned: its abundance marks the presence of a distributed, high-redundancy trophic network, its protective effects are species-specific and richness-independent, and preliminary evidence suggests context-dependent immune engagement consistent with resilience augmentation rather than simple anti-inflammatory activity[7].

## Methods

# Ethics and cohort

This study is a secondary analysis of data from the IHAT-GUT trial (ClinicalTrials.gov NCT02941081), a three-arm randomised controlled trial conducted November 2017–November 2018 in the Upper River

Region, The Gambia. No new clinical trial was conducted for the present study: all data were collected during the original trial, under the ethics approvals described below, and the present analyses were performed subsequently on the resulting anonymised dataset. The study protocol was approved by The Gambia Government/MRC Joint Ethics Committee (reference SCC1489), with Clinical Trials Authorisation from the Medicines Control Agency, The Gambia. The trial was conducted in accordance with the Declaration of Helsinki and ICH Good Clinical Practice guidelines. Written informed consent was obtained from parents or legal guardians prior to enrolment. Primary clinical trial findings are reported in Mohammed et al. (2023)[16]. Stool samples from 633 children aged 6–35 months with complete microbiome and adverse event data were included after quality-control exclusions and removal of antibiotic-treated participants. Iron treatment had no significant effect on microbiome composition or adverse event incidence and was not included as a covariate[6]. Full methodological details are described in de Goffau et al. (2022)[5] and Ofordile et al. (2025)[6]. This study adheres to the STROBE guidelines for observational reporting.

## Data preprocessing

Microbiome data and clinical metadata were derived from IHAT-GUT stool samples collected at Days 1 (D1), 15 (D15), and 85 (D85). Species-level relative abundances of *Prevotella stercorea* and *P. copri* were log-transformed ($\log_{1+}$). Genus-level richness was defined as the number of genera with abundance > 0 per sample. Shannon diversity was calculated as $H' = -\Sigma(p_i \log p_i)$. Inflammatory biomarkers (CRP, AGP) were log-transformed prior to modelling. Adverse event data were summarised per participant as total frequency (capped at five episodes) and cumulative duration (capped at 30 days) over the 113-day follow-up. Acute respiratory infection (ARI) was defined as clinician-diagnosed acute illness with cough and/or difficulty breathing, consistent with WHO/IMCI criteria.

# Statistical analysis

Group comparisons used two-sided Welch's t-tests with Cohen's *d* effect sizes. Discriminatory performance was assessed by receiver-operating characteristic (ROC) analysis (pROC package), with AUC compared using DeLong's test. Negative binomial generalised linear models (glm.nb, MASS package) were used for ARI frequency analyses, adjusted for age, sex, and height-for-age Z-score (HAZ). Species specificity was assessed in a joint model including *P. stercorea* and *P. copri* simultaneously. Mediation of the *P. stercorea*–ARI association by genus-level richness was evaluated using the product-of-coefficients approach ($a \times b$). WAZ-stratified linear models (median split) and continuous interaction terms (*P. stercorea* × WAZ) were used for inflammatory biomarker outcomes (log CRP, log AGP), adjusted for HAZ, age at sampling, and sex.

# Multiple testing correction

Where multiple comparisons arose within an analytical block, Benjamini–Hochberg (BH) false discovery rate correction was applied using p.adjust(method = "BH") in R. For the WAZ-stratified biomarker

analyses (Fig. 2d), two pre-specified correction families were defined: Family 1, comprising eight stratum-level association tests (D85 and D1 × CRP and AGP × Low and High WAZ); and Family 2, comprising four WAZ × *P. stercorea* interaction tests (D1 CRP, D1 AGP, D85 CRP, D85 AGP). BH-corrected interaction q-values are displayed in Fig. 2d; stratum-level q-values are reported in Supplementary Tables 6 and 7.

# Timepoint rationale for biomarker analyses

Inflammatory biomarkers (CRP, AGP) were measured at Day 1 for primary mechanistic analyses. This ensures a temporally antecedent immune state relative to the Day 85 microbiome exposure window, reducing reverse causation. Day 85 biomarker associations are presented for completeness but should be interpreted cautiously, as microbiome composition at this stage partially reflects illness status.

# Spaceflight analysis

Spaceflight analyses integrate published longitudinal microbiome data from Voorhies et al. (2019)[8], which profiled eight astronauts across five mission phases (pre-flight, early flight, mid-flight, late flight, and post-flight). Alpha diversity trajectories were expressed as percentage change from pre-flight baseline. Convergence dynamics were assessed descriptively: individuals with lower baseline diversity increase during flight while higher-baseline individuals remain stable, producing convergence toward a shared in-flight ecological state; variation reflects inter-individual differences. $Log_2$ fold-change values for key taxa were derived from the published dataset; taxa were selected based on established immunological relevance, including short-chain fatty acid producers and mucin-associated taxa. Simulated trajectories representing divergence between alpha diversity and functional microbial capacity used piecewise deterministic functions across mission phases; this is a conceptual framework illustrating that diversity convergence may co-occur with functional redundancy loss. Immune changes were summarised from published metrics including cytokine elevation (IL-1β, IL-2, IL-8) and viral reactivation (varicella zoster virus); data are descriptive and not re-analysed statistically.

# Conceptual ecological modelling

Stability landscape, redundancy–richness, and perturbation recovery models (Figs. 3c, 4) are theoretical and not subject to statistical inference. An asymmetric double-well potential models alternative stable microbiome states as a function of richness, with distinct attractors representing industrialised and non-industrialised configurations. Empirical richness distributions from the IHAT-GUT cohort were used to position populations along the conceptual functional redundancy gradient. Perturbation recovery trajectories were modelled under low- and high-redundancy regimes using deterministic perturbation functions, capturing tipping-point behaviour and incomplete recovery in the low-redundancy case. Recovery time was modelled as a nonlinear function of perturbation magnitude, diverging beyond a critical threshold to represent the qualitative shift in resilience that accompanies contraction below a minimum viable richness.

# Software

All statistical analyses were conducted in R (v4.5.0; R Core Team) using the *tidyverse*, *MASS*, *broom*, *pROC*, and *lme4* packages. Figures were assembled with *ggplot2* and *patchwork*. The complete analysis pipeline, including all EcologyTables_MASTER.R and figure generation scripts, is archived at https://github.com/ofordile-star/western-microbiome-fragility.

## Declarations

# Competing Interests

O.O. is Founder and CEO of Stercora Biosciences Inc., a company developing Prevotella stercorea as a therapeutic, postbiotic, and diagnostic platform. The IHAT-GUT data and all analyses reported in this manuscript were completed independently of Stercora Biosciences. No funding from Stercora Biosciences supported this work.

# Funding

The IHAT-GUT study was supported by a Bill & Melinda Gates Foundation Grand Challenges New Interventions in Global Health award (OPP1140952). The Nutrition Group of the MRC Unit The Gambia at LSHTM is supported by core funding from the UK Medical Research Council and the UK Department for International Development under the MRC/DFID Concordat agreement. The funders had no role in study design, analysis, manuscript preparation, or the decision to publish. This study received no specific funding. All analyses were conducted as an independent scholarly contribution by the author.

# Author Contribution

O.O. conceived the study, developed the theoretical framework, performed the analyses, interpreted the findings, and wrote the manuscript.

# Acknowledgement

I thank the staff of the MRC Unit The Gambia at the London School of Hygiene & Tropical Medicine (LSHTM), particularly Mr. Bakary Baldeh, the IHAT-GUT Nurse Coordinator, and the study nursing and field teams for their dedication to participant care, adverse-event monitoring, and data collection. I am also grateful to the staff of Yorrobawol Health Centre, Darsilami Community Health Post, Konkuba Community Health Post, Taibatu Health Post, and Chamoi Health Centre for supporting the study, and to the participating communities and families in the Wuli and Sandu districts of the Upper River Region, The Gambia.

# Data Availability

The datasets analysed during the current study are available on https://data.mendeley.com/datasets/fr5p4cgc7j/2. Raw bacterial 16S rRNA sequence data have been deposited in the European Nucleotide Archive (ENA) under accession number ERP110905. Spaceflight microbiome data from Voorhies et al. (2019) are available at the NASA Life Sciences Data Archive (lsda.jsc.nasa.gov).

# Code Availability

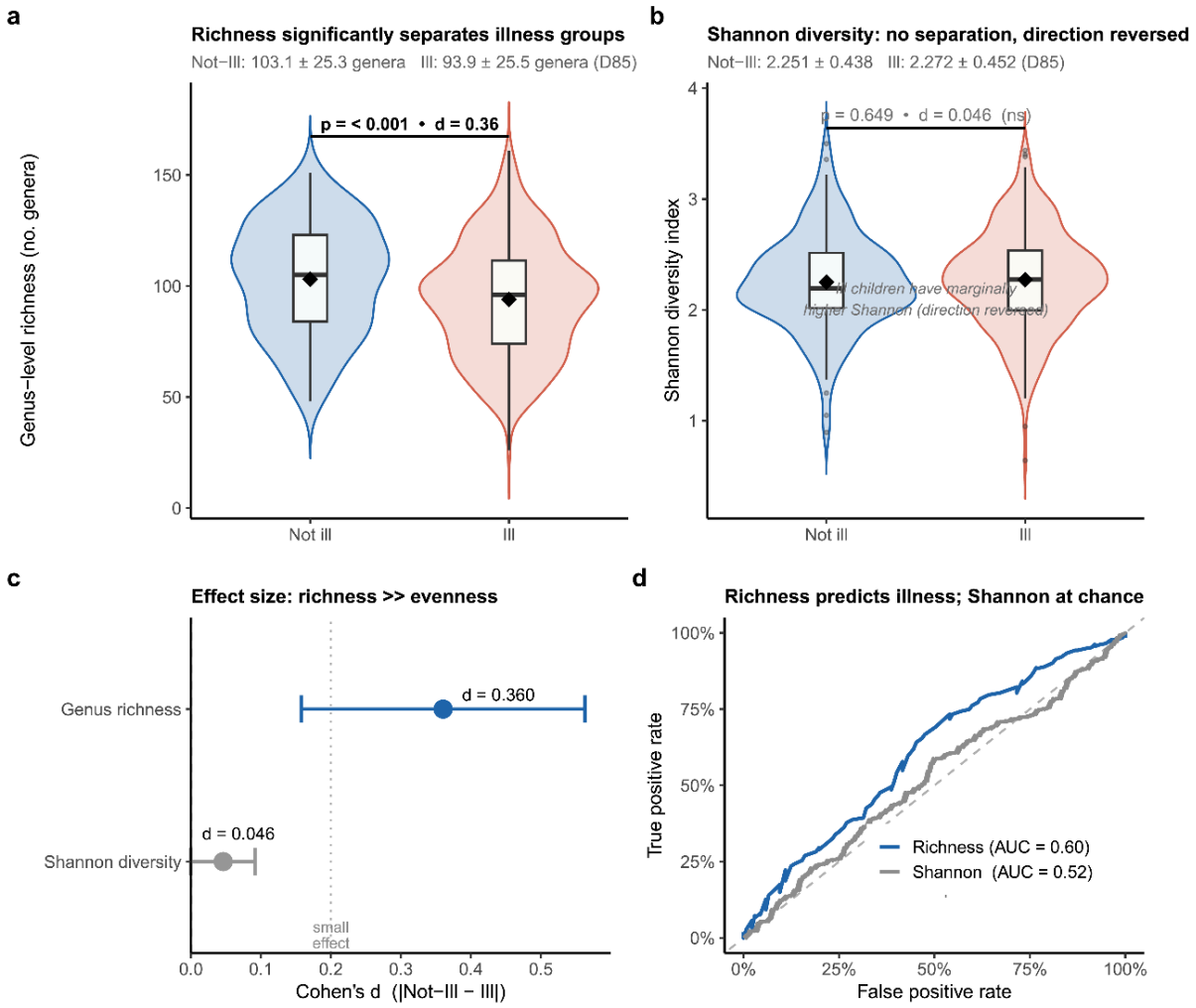
Analysis code and figure generation scripts are publicly available at https://github.com/ofordile-star/western-microbiome-fragility and will be formally archived at Zenodo upon acceptance.

## References


1. Holling, C. S. Resilience and stability of ecological systems. *Annu. Rev. Ecol. Syst.* **4**, 1–23. https://doi.org/10.1146/annurev.es.04.110173.000245 (1973).
2. Scheffer, M. et al. Early-warning signals for critical transitions. *Nature* **461**, 53–59. https://doi.org/10.1038/nature08227 (2009).
3. Arumugam, M. et al. Enterotypes of the human gut microbiome. *Nature* **473**, 174–180. https://doi.org/10.1038/nature09944 (2011).
4. Yatsunenko, T. et al. Human gut microbiome viewed across age and geography. *Nature* **486**, 222–227. https://doi.org/10.1038/nature11053 (2012).
5. de Goffau, M. C. et al. Gut microbiomes from Gambian infants reveal the development of a non-industrialised. *Nat. Microbiol.* **7**, 132–144. https://doi.org/10.1038/s41564-021-01023-6 (2022).
6. Ofordile, O. et al. Gut. *associates Prot. against Infect. rural Afr. Child. Nat. Commun.* **16**, 11101. https://doi.org/10.1038/s41467-025-66011-4 (2025).
7. Ofordile, O. Prevotellastercorea links gut microbiome ecology to respiratory infection protection through a host-context-dependent, species-autonomous pathway. [Under review, *BMC Medical* Genomics, 2026]. medRxiv doi:10.64898/2026.05.26.26354151[Preprint].
8. Voorhies, A. A. et al. Study of the impact of long-duration space missions at the International Space Station on the astronaut microbiome. *Sci. Rep.* **9**, 9911. https://doi.org/10.1038/s41598-019-46303-8 (2019).
9. Mehta, S. K. et al. Latent virus reactivation in astronauts on the International Space Station. *NPJ Microgravity*. **3**, 11. https://doi.org/10.1038/s41526-017-0015-y (2017).
10. Crucian, B. E. et al. Plasma cytokine concentrations indicate that in vivo hormonal regulation of immunity is altered during long-duration spaceflight. *J. Interferon Cytokine Res.* **34**, 778–786. https://doi.org/10.1089/jir.2013.0129 (2014).

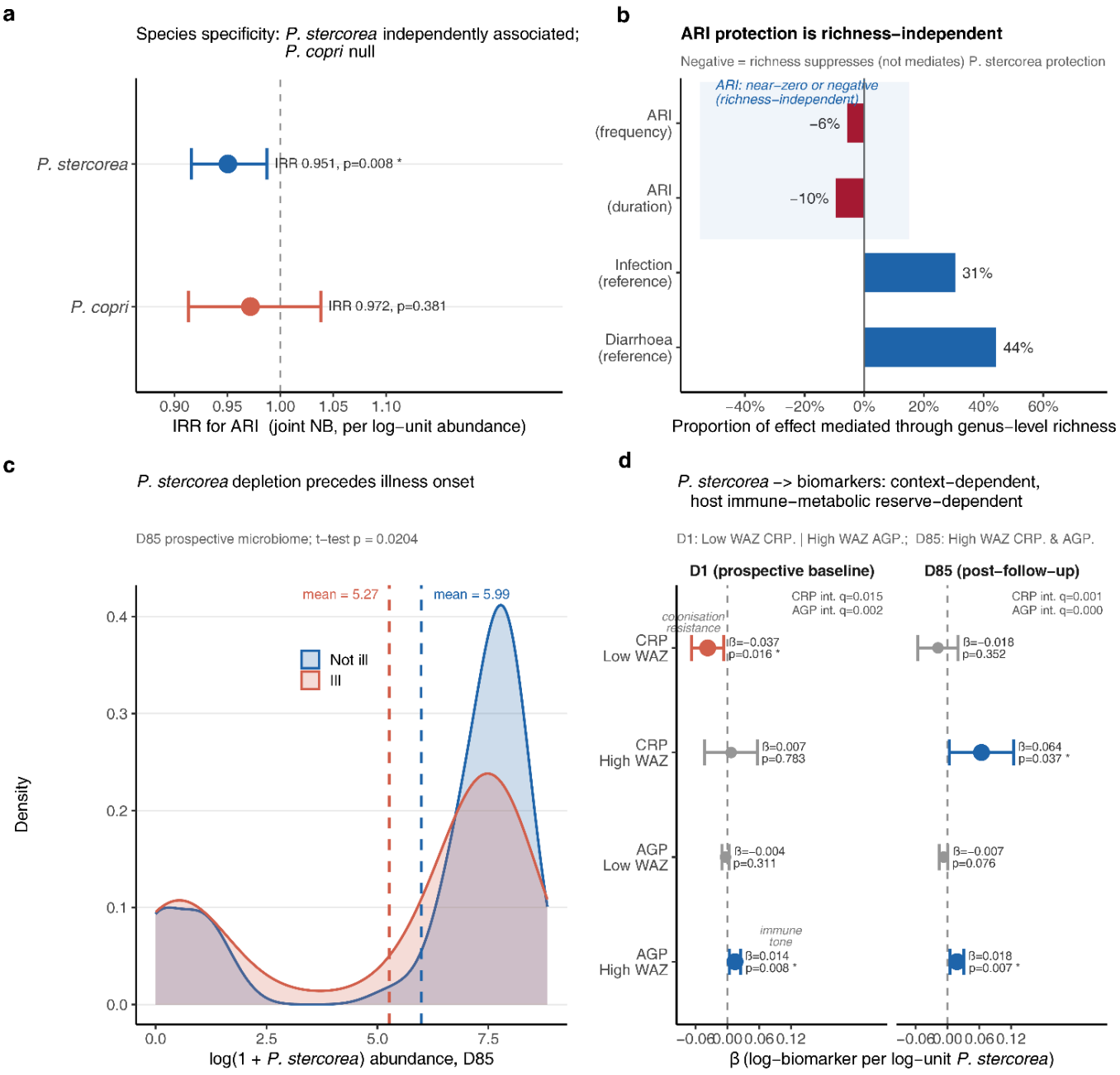
11. Blaser, M. J. & Falkow, S. What are the consequences of the disappearing human microbiota? *Nat. Rev. Microbiol.* **7**, 887–894. https://doi.org/10.1038/nrmicro2245 (2009).
12. Dang, A. T. & Marsland, B. J. Microbes, metabolites, and the gut–lung axis. *Mucosal Immunol.* **12**, 843–850. https://doi.org/10.1038/s41385-019-0160-6 (2019).
13. Wypych, T. P., Wickramasinghe, L. C. & Marsland, B. J. The influence of the microbiome on respiratory health. *Nat. Immunol.* **20**, 1279–1290. https://doi.org/10.1038/s41590-019-0451-9 (2019).
14. Jeyanathan, M. et al. Parenteral BCG vaccine induces lung-resident memory macrophages and trained immunity via the gut–lung axis. *Nat. Immunol.* **23**, 1687–1702. https://doi.org/10.1038/s41590-022-01339-7 (2022). (Note: exact DOI confirmed via standard Nature sources for this citation).
15. Wipperman, M. F. et al. Antibiotic treatment for tuberculosis induces a profound dysbiosis of the microbiome that persists long after therapy is completed. *Sci. Rep.* **7**, 10767. https://doi.org/10.1038/s41598-017-10346-6 (2017).
16. Mohammed, N. I. et al. A novel nano-iron supplement versus standard treatment for iron deficiency anaemia in children 6–35 months (IHAT-GUT trial): a double-blind, randomised, placebo-controlled non-inferiority phase II trial in The Gambia. *EClinicalMedicine* **9**, 56. https://doi:10.1016/j.eclinm.2023.101853 (2023).
17. Ofordile, O. Prevotella stercorea defines dual ecological pathways linking the gut microbiome to infection susceptibility. *Mendeley Data*. **V2** 10.17632/fr5p4cgc7j.2 (2026).

# Figures




## Figure 1

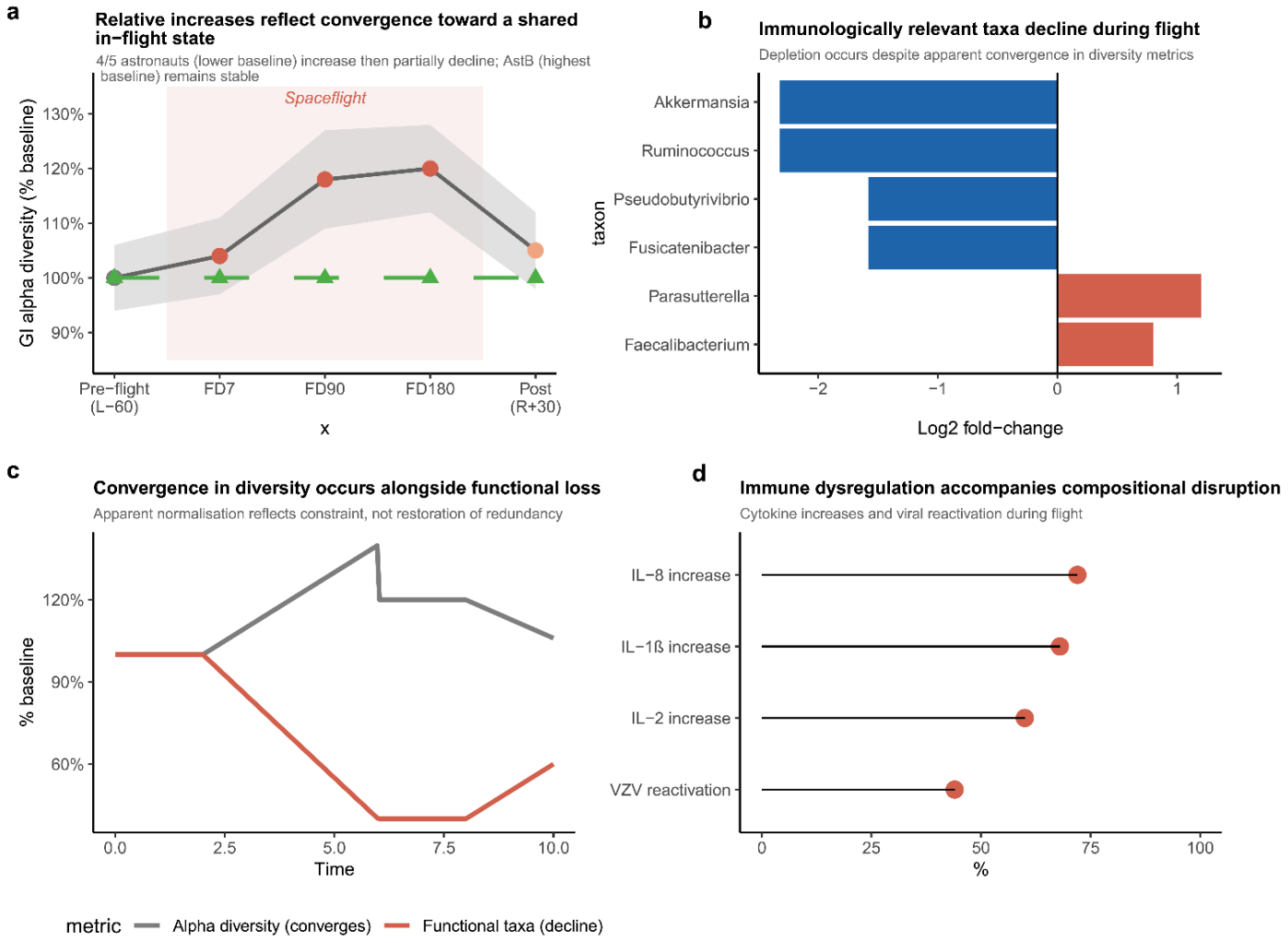
**Genus-level richness, but not Shannon diversity, associates with protection from infection**. **a,** Day 85 genus-level richness in children who remained infection-free versus those who developed illness (103.1 ± 25.3 vs 93.9 ± 25.5 genera; $p$ = 0.0005, Cohen's $d$= 0.36). Diamonds indicate group means. **b,** Shannon diversity showing no significant association with illness status and a directionally reversed trend (2.251 ± 0.439 vs 2.272 ± 0.452; $p$ = 0.649). **c,** Effect size comparison across diversity metrics. **d,** Receiver-operating characteristic curves for genus richness (AUC 0.605, 95% CI 0.548–0.662) and Shannon diversity (AUC 0.521, 95% CI 0.463–0.578). IHAT-GUT cohort ($n$ = 452; 137 not-ill, 315 ill). See Supplementary Tables 1 and 2.




## Figure 2

**Prevotella stercorea independently associates with reduced infection risk**. **a**, Adjusted incidence rate ratios from joint models (P. stercorea: IRR 0.951, 95% CI 0.916–0.987, p = 0.008; P. copri: IRR 0.972, p = 0.381; r = 0.32). See Supplementary Tables 3 and 4. **b**, Mediation analysis showing <1% of the association explained by genus-level richness. See Supplementary Table 5. **c**, Distribution of Day 85 P. stercorea abundance by illness group (means: 5.99 vs 5.27). **d**, Associations with CRP and AGP stratified by WAZ (low WAZ n = 200; high WAZ n = 84) at Day 1 and Day 85, with BH-corrected interaction q-values indicated (Family 2: four WAZ × P. stercorea interaction tests). Stratum-level annotations show raw p-values. D85 High WAZ CRP (n = 84; q = 0.075, BH Family 1: eight stratum-level tests) narrowly missed the BH threshold; all other stratum-level associations significant at raw p < 0.05 remain significant after BH

correction (q < 0.05). Host immune-metabolic reserve-dependent response pattern. See Supplementary Tables 6 and 7.




## Figure 3

**Convergence of diversity under constraint during spaceflight**. **a**, Longitudinal alpha diversity showing increases relative to baseline in 4/5 astronauts (Shannon p = 0.011; richness p = 0.05), primarily among those with lower pre-flight diversity; highest-diversity individual remains stable. **b**, Differential abundance (log2 fold-change) showing depletion of Akkermansia, Ruminococcus, Pseudobutyrivibrio, and Fusicatenibacter. **c**, Evidence of convergence toward a shared in-flight profile, followed by partial decline later in the mission. **d**, Immune correlates: inverse association between Fusicatenibacter and cytokines; viral reactivation in 44% of astronauts.

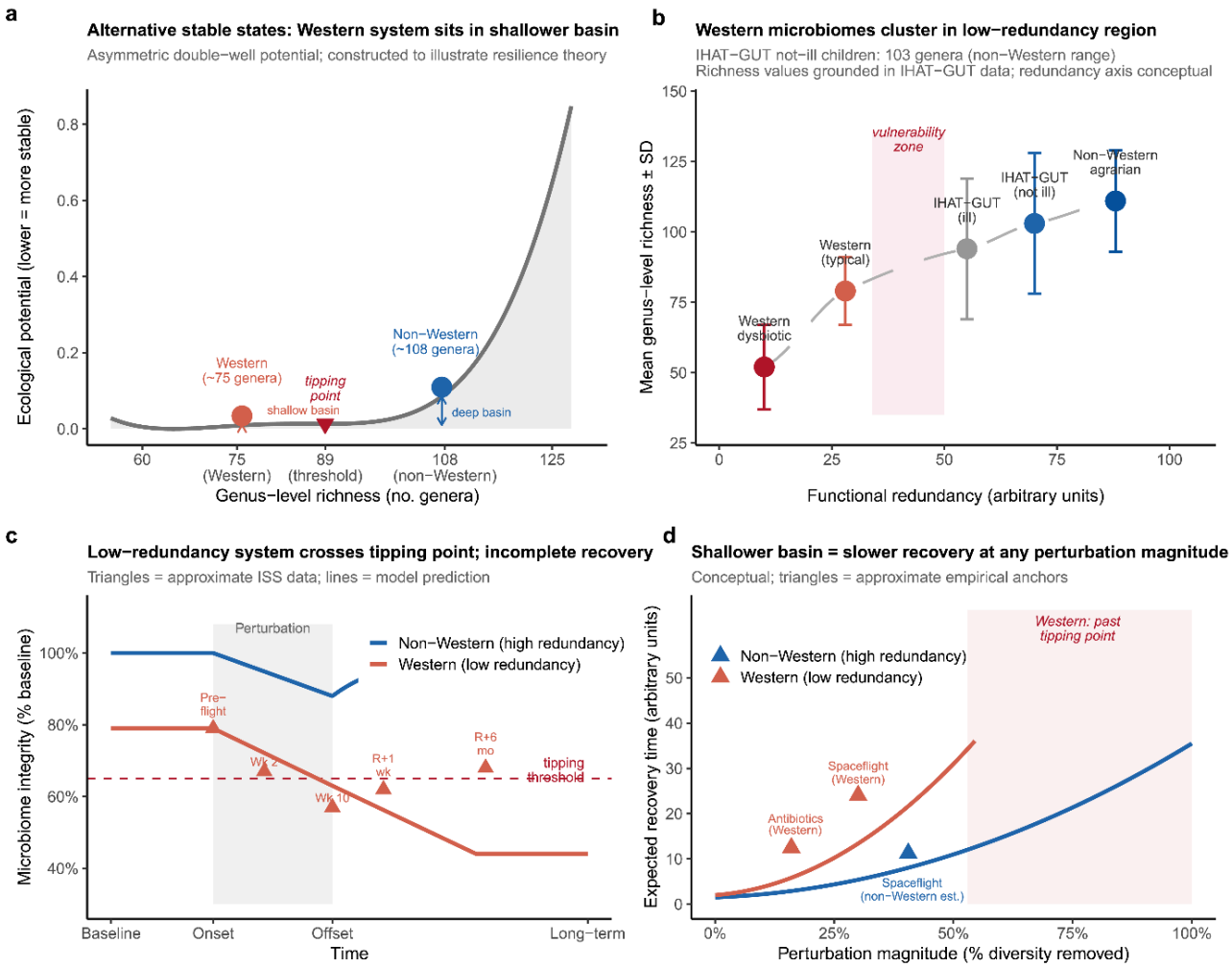



**Figure 4**

**Conceptual model of microbiome resilience and tipping points**. **a**, Stability landscape showing high- and low-richness attractors separated by a tipping point. **b**, Position of populations along a richness gradient (IHAT-GUT reference values shown; see Table 1). **c**, Predicted responses to perturbation in high- versus low-redundancy systems. **d**, Recovery dynamics illustrating reduced resilience in low-richness microbiomes.

# Supplementary Files

This is a list of supplementary files associated with this preprint. Click to download.

- EcoCollapsesupp.docx